Journal of Applied Polymer Science

Orthogonal design preparation of phenolic fiber by melt electrospinning

Gai Xie,[1] Zhiyuan Chen,[1] Seeram Ramakrishna,[2] Yong Liu[1]

[1]College of Mechanical and Electric Engineering, Beijing University of Chemical Technology, Beijing 100029, China
[2]Nanoscience and Nanotechnology Initiative, National University of Singapore, Singapore 117576, Singapore
Correspondence to: Y. Liu (E-mail: yongsd@iccas.ac.cn)

ABSTRACT: Through orthogonal experimental methods, the melt electrospinning of pure phenolic fibers has been achieved. The preparation is based on an orthogonal experimental method, which was designed to investigate the optimal conditions for production through integrated effects of spinning temperature, gap between spinneret and collector, as well as applied voltage. We found that optimal spinning conditions at 160°C, a spinneret-to-collector gap of 8 cm, and applied voltage at 40 kV produce an average electrospun fiber diameter reaching 4.44 ± 0.76 μm, with narrow variance distribution. The fibers were cured in a solution with 18.5% formaldehyde and 12% hydrochloric acid, heated from room temperature to 80°C and maintained 1h. In this report, the morphology, structural changes, and heat resistance of the fibers are characterized. Obtained results reveal that curing the fiber reduces crystallization and improves heat resistance. © 2015 Wiley Periodicals, Inc. J. Appl. Polym. Sci. **2015**, *132*, 42574.

KEYWORDS: crystallization; electrospinning; fibers; manufacturing; thermal properties

Received 4 March 2015; accepted 3 June 2015
DOI: 10.1002/app.42574

INTRODUCTION

Phenolic fibers were invented by Economy in 1972 and are used for aerospace insulation materials.[1] Owning to their extraordinary flame, heat and corrosion resistance, high carbonation rate, high carbon yield, as well as cheap and readily available raw materials, phenolic fibers have been widely used in many fields such as bunker clothing, fire-proof plates, anti-friction components, corrosion resistant fabric, sound insulation, composites, as precursors for carbon fibers and activated carbon.[2–5] Phenolic fibers are usually prepared by solution spinning or melt spinning. However, the obtained fibers always have a large diameter and the preparation process too is complicated.[6,7] With the development of modern technology, the need for thinner flame retardant fibers is ever increasing for nano- and micro-electronic devices. Phenolic fibers are a good candidate to meet this requirement.

Electrospinning is one of the most straightforward and simplest methods for forming continuous nano- to micro-scale fibers by forcing the materials through a spinneret under the effect of an electric field, then depositing fibers on a collector.[8,9] This method can be divided into solution electrospinning and melt electrospinning according to the different states of the spinning materials. Many researchers combined electrospinning techniques in various studies.[10–12] In recent years, phenolic fibers have been produced primarily by solution electrospinning.[13–15] These studies greatly promoted the development of phenolic fibers. However, there are still some drawbacks. Firstly, residual solvent in the fibers could cause defects within the fibers and then affect their physical properties.[16,17] Secondly, preparation of phenolic fibers by solution electrospinning requires additives to improve the viscosity of the spinning solution for the low molecular weight, but the additives, such as polyvinylpyrrolidone (PVP), a nonheat-resistant polymer, would reduce thermal performance of the phenolic fibers.[15] Thirdly, the additives used in solution electrospinning to prepare phenolic fibers include $NaCO_3$, Pyridine, ethanol, surfactant, PVP, Poly(vinyl alcohol) (PVA), and so on.[2,5,13–15,18,19] Adding the additives to improve the viscosity and electrical conductivity of the spinning solution is a complex process. Finally, the fiber production is very low in solution electrospinning. However, to the best of our knowledge, only Gee's patents described the preparation of phenolic fibers through melt electrospinning. The patents involve the melt phenolic polymeric system, molecular weight, as well as the performance of the obtained fibers, while include little detailed discussion on the structure and properties of the resulting fibers.[16,17] Compared with solution electrospinning, melt electrospinning, forms fibers directly from heated polymer in the absence of solvents, is considered to be a greener and simpler way, which process avoids the pollution and damage of toxic solvents. The fibers have fewer defects and better physicomechanical properties besides higher throughput.[18]

Orthogonal experimental design is a mathematical method used for arranging multifactor, multilevel experiments, in which

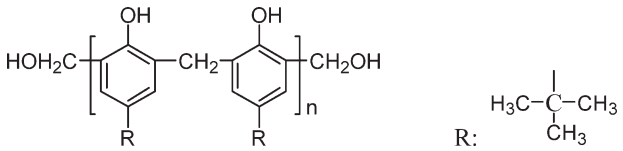

Scheme 1. The formula of para-tert-butylphenol formaldehyde resin.

representative points are selected to carry out sample experiments from the overall experiments on the basis of orthogonality. This scientific and efficient method is applied broadly in many fields to investigate the relative importance of each factor and identifies the ideal values for various factors.[21–26] We can quickly determine the impact of factors and their levels by employing the orthogonal experimental design method, which not only saves experimental time and raw materials, but also provides accurate and credible optimal parameters, in this case, for melt electrospinning.

In view of the facts mentioned above, we used melt electrospinning to generate pure phenolic fibers, based on an orthogonal experimental design. As well, fiber characteristics such as crystallization and heat resistance were evaluated.

EXPERIMENTAL

Materials and Equipment

The analytical-grade powder of para-tert-butylphenol formaldehyde resin was used without further purification as the raw material for melt electrospinning. The resin was purchased from Letai Chemical (China). The weight average molecular weight ($\overline{M_w}$) = 2733 g·mol^{-1} and the number average molecular weight ($\overline{M_n}$) = 1968 g·mol^{-1} of the received para-tert-butylphenol formaldehyde resin were measured by gel permeation chromatography (GPC, Waters 1525, America). Tetrahydrofuran was used as the solvent for GPC analysis, the column temperature was 35°C, the injection volume was 50 μL and the flow rate was 2.5 μL·min^{-1}. The formula of para-tert-butylphenol formaldehyde resin was given in Scheme 1. The melt electrospinning device used here

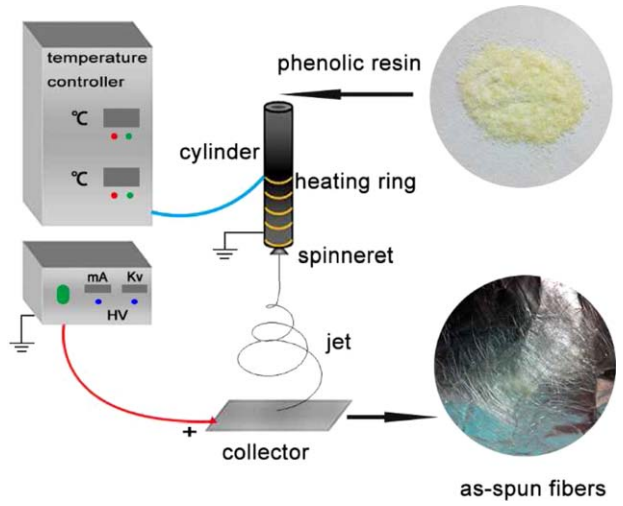

Figure 1. Schematic diagram of the melt electrospinning process. [Color figure can be viewed in the online issue, which is available at wileyonlinelibrary.com.]

was the same as that used in our previous research.[27–29] The schematic diagram of the electrospinning process is shown in Figure 1. The collector was connected to the positive high-voltage power-supply terminal, and the spinneret was grounded. All experiments were carried out at room temperature.

Experimental Arrangement

Well-established factors affecting melt electrospun fiber diameter and distribution include molecular structure, spinning temperature, voltage, spinning distance, and melt flow rate.[30–34] Each of these factors has different effects. In the present study, an orthogonal design table $L_9(3)^4$ were designed using the software, Orthogonal Designing Assistant II (Sharetop Software Studio, v3.1). Typically each orthogonal table has its own mark denoted as $L_n(t)^c$, L represent the orthogonal table, the number lower right corner of L is the total number of experiments, t is the number of levels of each factors, the superscript (c), representing the maximum allowed number of factors. The factors of spinning temperature, distance between the spinneret and the collector and applied voltage (called hereafter: temperature, distance, and voltage) labeled as A, B, and C were investigated.[26] On the basis of the previous experiments, it was determined that viscosity of phenolic resins is too high for melt electrospinning lower than 140°C, leading to very low spinning efficiency. However, when the spinning temperature is above 160°C, serious degradation of phenolic resins occurred in the melt electrospinning process. Simultaneously taking into account the needs for relatively high electric field strength in melt electrospinning, levels corresponding to each factor are shown in Table I.

Characterization

The morphology of the phenolic fibers was characterized by scanning electron microscope (SEM, Hitachi SU1510, Japan), and each sample was gold coated prior to imaging. The fiber diameters were calculated from the SEM images by using Image J software (NIH, USA). Twenty different fibers were randomly selected, and five different points on each fiber were measured from each image. The crystallization of the fibers was examined using an x-ray diffraction (XRD, D8 Focus, Bruker, Germany) in the 2θ range of 4–60° with Cu Kα (λ = 1.5406 Å) having voltage 40 kV and current 40 mA. The equipment resolution and the scan speed were 0.02° and 0.1 s/step, respectively. For curing, the obtained fibers were immersed in a mixed solution of 18.5% formaldehyde with 12% hydrochloric acid, then oven-dried from room temperature to 80°C at an average rate of 10°C·h^{-1}.[35] The fibers were then maintained at 80°C for 1 h. Next, the cured fibers were washed with distilled water and then dried at room temperature. Fourier transform infrared

Table I. Factors and Levels for Orthogonal Experimental Design

	Factors		
Levels	A (°C)	B (cm)	C (kV)
1	140	8	30
2	150	9	35
3	160	10	40

Table II. Results and Analysis of Orthogonal $L_9(3)^4$ Experimental Design

	Factors			Results	
Experiment No.	A (°C)	B (cm)	C (kV)	Average diameter (μm)	SD of average diameter
1	1	1	1	15.43	13.02
2	1	2	2	21.36	2.03
3	1	3	3	10.44	1.58
4	2	1	2	6.36	0.92
5	2	2	3	3.42	2.85
6	2	3	1	18.64	8.94
7	3	1	3	4.44	0.76
8	3	2	1	7.04	4.06
9	3	3	2	11.88	2.41

	A	B	C	A	B	C
K_1	15.74	8.74	13.70	5.54	4.90	8.67
K_2	9.47	10.61	13.20	4.24	2.98	1.79
K_3	7.79	13.65	6.10	2.41	4.31	1.73
R	7.95	4.91	7.60	3.13	1.92	6.94
Order of Importance	A > C > B			C > A > B		
Optimal level	A3	B1	C3	A3	B2	C3

SD means standard deviation.

$K_l^F = (\sum$ the value of evaluation indexes at the same level of each factor$)/3$

$R^F = \max\{K_l^F\} - \min\{K_l^F\}$

(F stands for factor A, B and C. l stands for levels 1, 2, and 3)

spectra were obtained on fourier transform infrared spectroscopy (FTIR, Nicolet 6700, Thermo Fisher, USA) with a resolution of 0.1 cm^{-1} at room temperature. For differential scanning calorimetry (DSC, Mettler-Toledo 800, Switzerland), measurement, the pan used is alumina, and the samples were heated from 25°C to 130°C at 10°C·min^{-1} in nitrogen (20 mL·min^{-1}) atmosphere. Thermogravimetric analysis (TGA) was carried out on a Netzsch Q500 thermoanalyzer between 40°C and 800°C at 10°C ·min^{-1} in nitrogen (50 mL·min^{-1}) atmosphere. FTIR, DSC, and TGA were employed to characterize the structure and heat resistance of the cured phenolic fibers.

RESULTS AND DISCUSSION

The Optimal Spinning Condition

Average diameter and standard deviation (SD) of average diameter were the evaluation indices of the orthogonal experiment in this study. K_1, K_2, and K_3 in Table II represent the mean values of evaluation indices for the three levels corresponding to the analyzed factors. For example, when the factor is B (distance), the level is 2 (9 cm) and the evaluation index is average diameter, then K_2 is calculated according to the following formula: $K_2 = (21.36 + 3.42 + 7.04) / 3 = 10.61$, which represents the mean value of average diameter for factor B at level 2. By comparing various K values, the optimal level of factors can be confirmed. On the other hand, R denotes range, which is the difference between the maximum and minimum K values. For instance, the R value for factor A of average diameter is: $15.74 - 7.79 = 7.95$. It reflects the effects of a conducive or detrimental level on the average diameter and its standard deviation. The maximum the R value corresponds to the most important factor.[36] Because thinner and uniform fibers can better meet the requirements of more fields, the value of K should be chosen as small as possible. Calculated on this basis, the analysis results are shown at the bottom of Table II. Figure 2 is drawn according to the K values of average diameter and SD of average diameter in Table II, illustrating that optimal level of each factor to obtain the fine fibers is A3, B1, and C3. It is noteworthy that the fiber diameters increase by increasing the distance in this study, which is different from the normal expectations to have finer fibers by increasing the spinning distance. Possible explanation for this phenomenon as follows: in

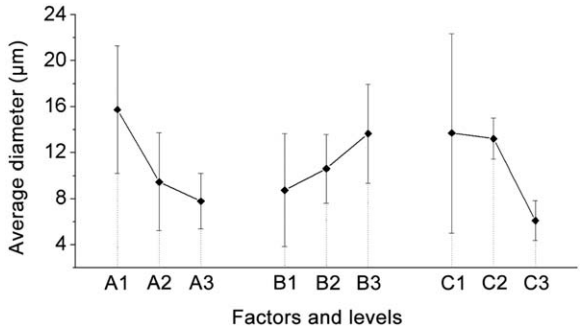

Figure 2. Relationship between average diameter with the three factors and levels.

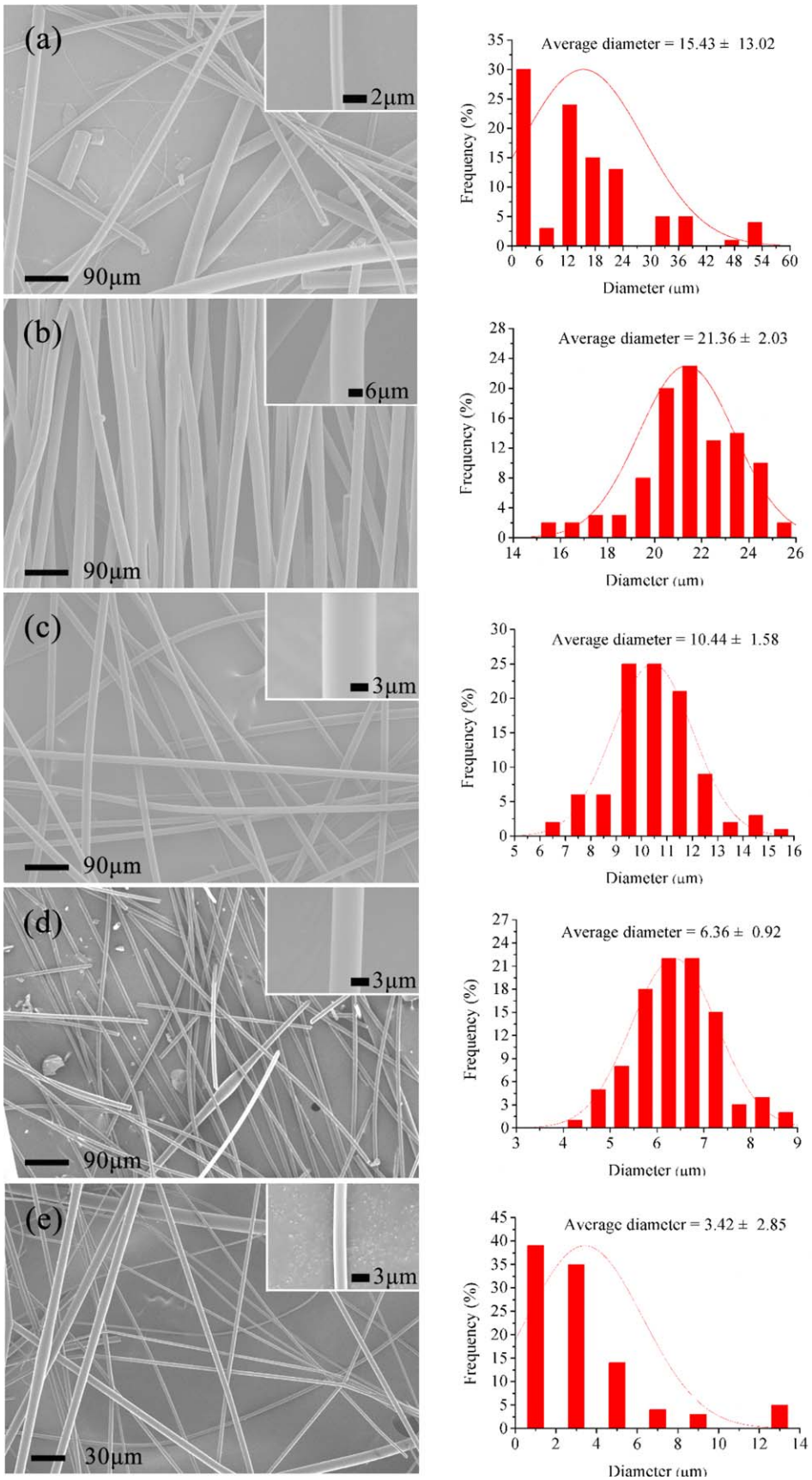

Figure 3. SEM images showing the morphology and diameter distribution of the as-spun phenolic fibers; (a)–(i) correspond to experiments 1–9, the histogram on the right were corresponding to the diameter distribution of each experiment. [Color figure can be viewed in the online issue, which is available at wileyonlinelibrary.com.]

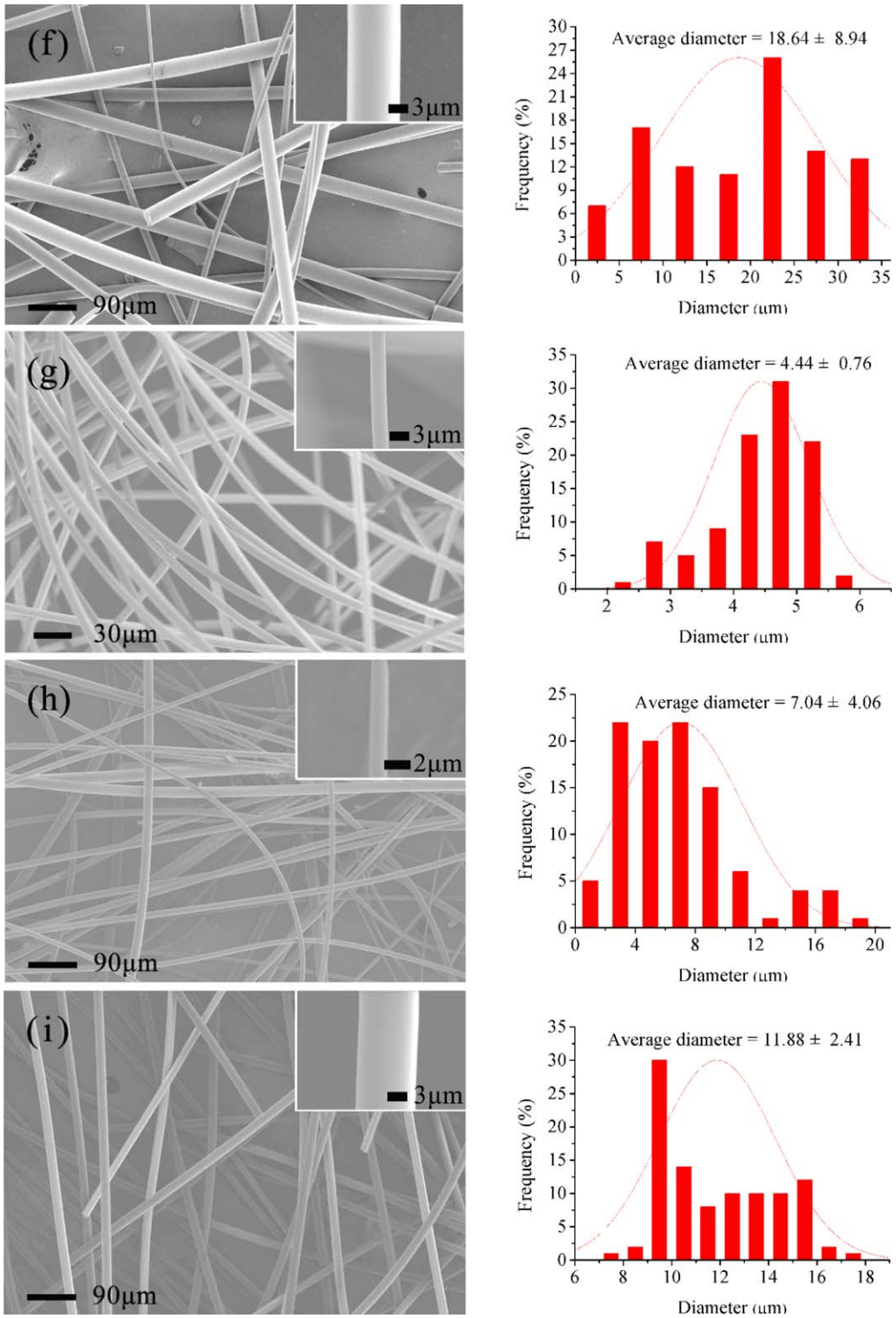

Figure 3. (Continued). [Color figure can be viewed in the online issue, which is available at wileyonlinelibrary.com.]

the orthogonal experiments, it is a comprehensive study of the effects of different levels of several factors. The temperature related to the melt viscosity, the distance, and the voltage related to the electric field strength. Additionally, compared to solution electrospinning, the polymer jets in melt electrospinning have higher viscosity, bigger diameter, and lower conductivity, so the impact of air turbulence of melt electrospinning is smaller than solution electrospinning. Therefore, the electric field strength plays the dominant role in the jet refinement process. But, in this orthogonal experiment, the voltage may be

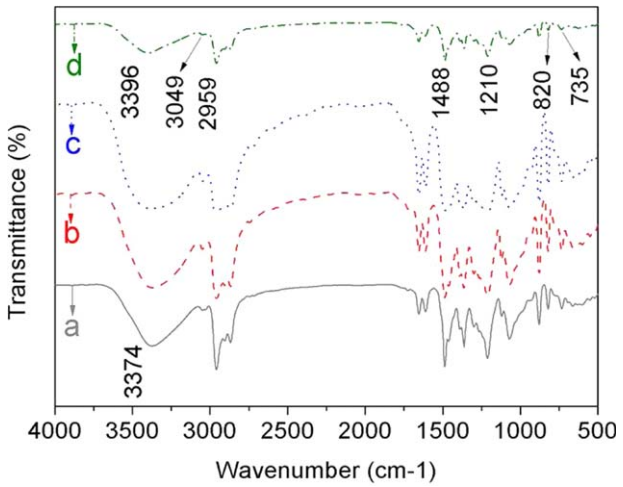

Figure 4. FTIR spectra of (a) phenolic resins, (b) phenolic resins dried in vacuum, (c) fibers electrospun from b, and (d) cured fibers from c. [Color figure can be viewed in the online issue, which is available at wileyonlinelibrary.com.]

decreased when the distance increased, thus reducing the electric field strength, which caused bigger Taylor cone and larger initial jet diameter. And the subsequent electric force still insufficient to significantly reduce the fiber diameter. Therefore, it is possible that the fiber diameter increases by increasing the distance in the orthogonal experiments. As a result, there is a need to consider the pair wise interactions between the three factors to fully understand the inter-relationship.

Figure 3 shows the SEM images from nine experiments in Table II. An image of the minimum diameter fiber in each case appears at the upright corner of the full SEM image. The histogram on the right shows the fiber diameter distribution of each experiment. These images suggest that phenolic fibers with a smooth surface were obtained successfully through melt electrospinning. From this set, image (g) of experiment 7 shows the best fiber morphology and most uniform fibers. Interestingly, experiment 7 corresponds exactly to the optimal condition, A3B1C3, in Table I. In addition, the average diameter under the optimal condition is 4.44 ± 0.76 μm, which is lower than that obtained using traditional melt spinning, although it is not the finest reported in melt electrospinning research.[14,20]

Heat Resistance and Crystallization of Fibers

In Figure 4 can be seen that the peak for aliphatic C–H (2959 cm^{-1}) of the phenolic resins dried in vacuum (curve b) becomes weak, when compared to raw materials (curve a), owing to the fact that free phenol and other small molecules in raw materials are excluded after drying. The intensity of peaks corresponding to aliphatic C–H (2959 cm^{-1}) and $–CH_2–$ methylene bridges (1488 cm^{-1}) decreases in the as-spun fibers (curve c), while increasing in the cured fibers (curve d).

In addition, compared with as-spun fibers, the intensity of the peak corresponding to the aromatic C–H stretch (3049 cm^{-1}), plus 1,4- and 1,2,4-substituted benzene rings (820 cm^{-1}) together with 1,2- and 1,2,6-substituted benzene rings (735 cm^{-1}), all decreased after curing (curve d). Moreover, the peak corresponding to phenolic –OH shifts to a higher wave number (3396 cm^{-1}), which means that the melting temperature (T_m) rose (curve d). A dehydration condensation reaction may have occurred between phenolic –OH(s) and methylene, causing the peak intensity corresponding to phenolic –OH to decrease and those corresponding to diphenyl ether (1210 cm^{-1}) and substituents of the benzene ring to increase, thereby enhancing the curing degree. On the other hand, the TGA analysis and the corresponding DTG curves are shown in Figure 5 on the left side and right side, respectively. The thermal characteristics such as onset decomposition temperature (T_{on}), 50% loss temperature ($T_{0.5}$), temperature at the maximum decomposition rate (T_{d1} and T_{d2}, peak obtained from DTG curves) and yield of charred residue at 800°C are shown in Table III. It can be seen that no considerable alteration in T_{d1} and T_{d2} are observed in all samples, but T_{on}, $T_{0.5}$, and the residue at 800°C of the as-spun fibers are lowest while highest for the cured fibers. This indicates that the decomposition of as-spun fibers is faster than the cured fibers. According to Bai, the difference in diameter has great influence on the thermal stability of fiber, and the degree of weight loss becomes observably higher during heating process with the diameter of fiber decreasing, so the as-spun fibers showed different behavior in TGA may also because of the fiber size.[13] But, it also might be

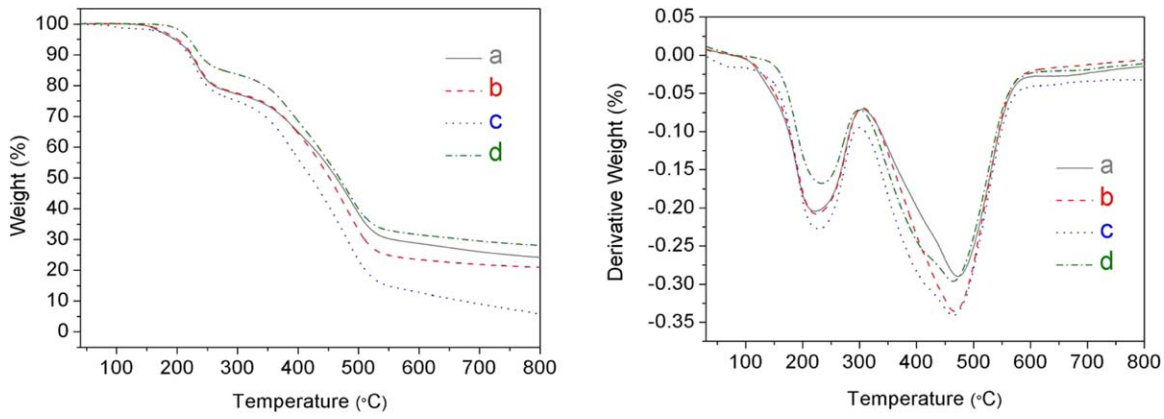

Figure 5. TGA analysis (left) and corresponding DTG curves (right) of (a) phenolic resins, (b) phenolic resins dried in vacuum, (c) fibers electrospun from b, and (d) cured fibers of c. [Color figure can be viewed in the online issue, which is available at wileyonlinelibrary.com.]

Table III. Thermal Characteristics of Phenolic Resins and Fibers

Curve	T_{on} (°C)	$T_{0.5}$ (°C)	T_{d1} (°C)	T_{d2} (°C)	Residue at 800°C (wt %)
a	150	470	221	475	24.0
b	150	456	221	468	21.0
c	76	425	226	466	6.5
d	185	474	230	465	28.5

a—Phenolic resins, b—Phenolic resins dried in vacuum, c—Fibers electrospun from b, d—Cured fibers of c.

because of the thermal history resulting from melt electrospinning, which caused the spun fibers shown different behavior in TGA. A part of molecular bonds might become weak because of the thermal history, and then these molecular bonds will quickly break down once heating again. These results suggest that the heat resistance of fibers improves a bit after curing although the degree of cure is not high.

As observed in Figure 6, T_m for the thermoplastic phenolic resin after vacuum-drying (curve b) falls slightly, while it increases for as-spun fibers (curve c). This probably because of the raw material used in this study was unpurified para-tert-butylphenol formaldehyde resin, in which contained small molecule and monomers. These small molecule and monomers in the raw material might act as a plasticizer. However, these plasticizers were volatilized during the melt electrospinning process because of high temperature and leaving long-chain molecule. Thus the increased content of long molecule chains resulting in slightly high melting temperature to the spun fibers.[37,38] Two unclear melting peaks marked in a rectangle box, which has been enlarged for display, appear for cured fibers (curve d). The peak at 65°C possibly because of more serious chain entanglement of cured fibers, which result in higher viscosity and cause restricted molecular chain movement, thereby leading to higher T_m.[37,38]

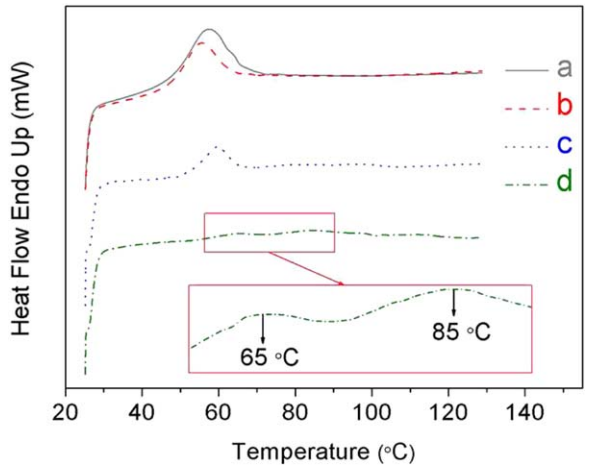

Figure 6. DSC curves of (a) phenolic resins, (b) phenolic resins dried in vacuum, (c) fibers electrospun from b, and (d) cured fibers from c. [Color figure can be viewed in the online issue, which is available at wileyonlinelibrary.com.]

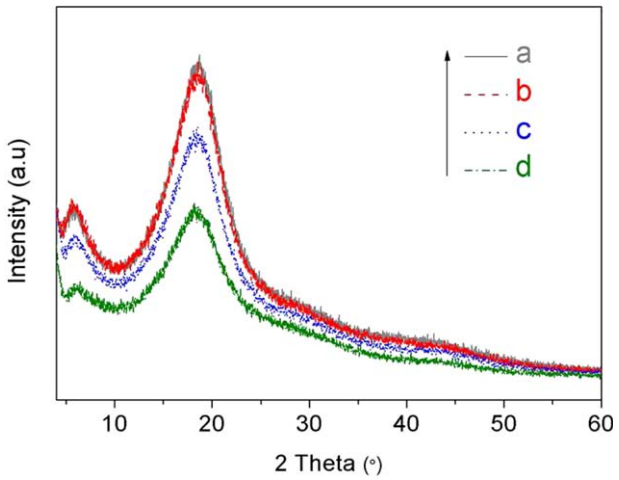

Figure 7. XRD curves of (a) phenolic resins, (b) phenolic resins dried in vacuum, (c) fibers electrospun from b, and (d) cured fibers from c. [Color figure can be viewed in the online issue, which is available at wileyonlinelibrary.com.]

Because of the exothermic heat from curing offsets part of the melting endothermic heat, the peak is flat. Additionally, an imperfect crystal structure results in recrystallization, origin of the peak at 85°C. Generally, the peaks of curve d are much smaller than those of curves a, b, and c, indicating reduced crystallization. The rise of peak temperature (curve d) indicates that the heat resistance improves in the cured fibers. The degree of crystallinity based on the XRD curves (Figure 7) were acquired by using software MDI jade 5.0 and keeping the error value below 9%. The final result was the average value of three calculations. The crystallinity corresponding to curves a, b, c, and d were 15.86%, 15.50%, 13.43%, and 11.73%. The decrease in relative intensity on XRD curve c also shows that the melt electrospinning process destroys the regularity of the molecular chain, which reduces crystallization. In addition, the decrease in the peaks of curve d indicates that the curing process further reduces crystallization.

CONCLUSIONS

In this research, pure phenolic fibers were prepared successfully by melt electrospinning. An orthogonal experimental design method was adopted to design the experiments. The order of importance for analyzed factors is temperature > voltage > distance. The optimal spinning conditions are a spinning temperature of 160°C, distance between the spinneret and the collector of 8 cm, and applied voltage of 40 kV. The average fiber diameter under this condition is 4.44 ± 0.76 μm, with a narrow diameter distribution. Pure phenolic fibers showed lower crystallization after curing; however, their heat resistance increased. Since the relative molecular mass of phenolic resins is not very high, their spinnability was relatively low. More in-depth studies of aspects such as the flame-retardant properties of the ultrafine phenolic fibers in this work are now in progress. With this orthogonal study, available quality in melt electrospun phenolic fiber has taken a step forward.

ACKNOWLEDGMENTS

This study was financially supported by the National Natural Science Foundation of China (21374008).

REFERENCES

1. Economy, J.; Clark, R. A. U.S. Patent 3,650,102, March 21, **1972**.
2. Wang, M. X.; Huang, Z. H.; Kang, F. Y.; Liang, K. M. *Mater. Lett.* **2011**, *65*, 1875.
3. Gugumus, F. *Polym. Degrad. Stab.* **1994**, *44*, 273.
4. Reghunadhan, N. C. P.; Bindu, R. L.; Ninan, K. N. *Polym. Degrad. Stab.* **2001**, *73*, 251.
5. Wang, L.; Huang, Z. H.; Yue, M. B.; Li, M. Z.; Wang, M. X.; Kang, F. Y. *Chem. Eng. J.* **2013**, *218*, 232.
6. Liu, C. L.; Ying, Y. G.; Feng, H. L.; Dong, W. S. *Polym. Degrad. Stab.* **2008**, *93*, 507.
7. Zhang, D. Q.; Shi, J. L.; Guo, Q. G.; Song, Y.; Liu, L.; Zhai, G. T. *J. Appl. Polym. Sci.* **2007**, *104*, 2108.
8. Lipka, J. K.; Gubanska, I.; Janik, H.; Sienkiewicz, M. *Mater. Sci. Eng. C Mater.* **2015**, *46*, 166.
9. Smyth, M.; Poursorkhabi, V.; Mohanty, A. K.; Gregori, S.; Misra, M. *J. Mater. Sci.* **2014**, *49*, 2430.
10. Pavliňák, D.; Hnilica, J.; Quade, A.; Schäfer, J.; Alberti, M.; Kudrle, V. *Polym. Degrad. Stab.* **2014**, *108*, 48.
11. Kancheva, M.; Toncheva, A.; Manolova, N.; Rashkov, I. *Mater. Lett.* **2014**, *136*, 150.
12. Zhang, C. L.; Yu, S. H. *Chem. Soc. Rev.* **2014**, *43*, 4423.
13. Bai, Y.; Huang, Z. H.; Kang, F. Y. *Carbon* **2014**, *66*, 705.
14. Ma, C.; Song, Y.; Shi, J. L.; Zhang, D. Q.; Zhai, X. L.; Zhong, M.; Guo, Q. G.; Liu, L. *Carbon* **2013**, *51*, 290.
15. Teng, M. M.; Qiao, J. L.; Li, F. T.; Bera, P. K. *Carbon* **2012**, *50*, 2877.
16. Karles, G. D.; Gee, D.; Wnek, G.; Layman, J.; Zhuang, M. E.P. Patent 2,004,080,217 A1, September 23, **2004**.
17. Karles, G. D.; Gee, D.; Wnek, G.; Layman, J.; Zhuang, M. U.S. Patent 8,012,399 B2, September 6, **2011**.
18. Ma, C.; Song, Y.; Shi, J. L.; Zhang, D. Q.; Zhong, M.; Guo, Q. G.; Liu, L. *Mater. Lett.* **2012**, *76*, 211.
19. Imaizumi, S.; Matsumoto, H.; Suzuki, K.; Minagawa, M.; Kimura, M.; Tanioka, A. *Polym. J.* **2009**, *41*, 1124.
20. Hutmacher, D. W.; Dalton, P. D. *Chem. Asian. J.* **2011**, *6*, 44.
21. Tehrani, A. H.; Zadhoush, A.; Karbasi, S.; Khorasani, S, N. *J. Appl. Polym. Sci.* **2010**, *118*, 2682.
22. Cui, W. G.; Li, X. H.; Zhou, S. B.; Weng, J. *J. Appl. Polym. Sci.* **2007**, *5*, 3105.
23. Liu, M. Z.; Cheng, Z. Q.; Jin, Y.; Ru, X.; Ding, D. W.; Li, J. F. *J. Appl. Polym. Sci.* **2013**, *130*, 3600.
24. Chen, S.; Wu, B. H.; Fang, J. B.; Liu, Y. L.; Zhang, H. H.; Fang, L. C.; Guan, L.; Li, S. H. *J. Chromatogr. A* **2012**, *1227*, 145.
25. Zheng, P. C.; Liu, H. D.; Wang, J. M.; Yu, B.; Zhang, B.; Yang, R.; Wang, X. M. *Anal. Methods* **2014**, *7*, 2163.
26. Wang, C. Q. Wang, H.; Liu, *Y. N. Waste Manage.* **2015**, *35*, 42.
27. Zhao, F. W.; Liu, Y.; Yuan, H. L.; Yang, W. M. *J. Appl. Polym. Sci.* **2012**, *4*, 2652.
28. Liu, Y.; Zhao, F. W.; Zhang, C.; Zhang, J. M.; Yang, W. M. *J. Serb. Chem. Soc.* **2012**, *8*, 1071.
29. Liu, Y.; Li, X. H.; Ramakrishna, S. *J. Polym. Sci. B Polym. Phys.* **2014**, *52*, 946.
30. Poursorkhabi, V.; Mohanty, A. K.; Misra, M. *J. Appl. Polym. Sci.* **2015**, *132*, 41260.
31. Kong, C. S.; Jo, K. J.; Jo, N. K.; Kim, H. S. *Polym. Eng. Sci.* **2009**, *49*, 391.
32. Andrzej, G.; Waclaw, T.; Wojciech, S.; Marek, S.; Michal, K.; Danuta, C. *J. Appl. Polym. Sci.* **2012**, *125*, 4261.
33. Zheng, Y. S.; Zeng, Y. C. *J. Mater. Sci.* **2014**, *49*, 1964.
34. Song, T. D.; Chen, Z. Y.; He, H.; Liu, Y. X.; Liu, Y.; Ramakrishna, S. *J. Appl. Polym. Sci.* **2015**, *132*, 41755.
35. Liu, C. L.; Guo, Q. G.; Shi, J. L.; Liu, L. *Mater. Chem. Phys.* **2005**, *90*, 315.
36. Alam, H. G.; Moghaddam, A. Z.; Omidkhah, M. R. *Fuel Process. Technol.* **2009**, *90*, 1.
37. Uslu, İ.; Tunç, T.; Keskin, S.; Öztürk, M. K. *Fiber. Polym.* **2011**, *12*, 303.
38. Ding, B.; Kim, H. Y.; Lee, S. C.; Lee, D. R.; Choi, K. *J. Fiber. Polym.* **2002**, *3*, 73.